Cell

Excess Membrane Synthesis Drives a Primitive Mode of Cell Proliferation

Romain Mercier,[1,2] Yoshikazu Kawai,[1,2] and Jeff Errington[1,*]
[1]Centre for Bacterial Cell Biology, Institute for Cell and Molecular Biosciences, Medical School, Newcastle University, Richardson Road, Newcastle upon Tyne NE2 4AX, UK
[2]These authors contributed equally to this work
*Correspondence: jeff.errington@ncl.ac.uk
http://dx.doi.org/10.1016/j.cell.2013.01.043

SUMMARY

The peptidoglycan cell wall is a hallmark of the bacterial subkingdom. Surprisingly, many modern bacteria retain the ability to switch into a wall-free state called the L-form. L-form proliferation is remarkable in being independent of the normally essential FtsZ-based division machinery and in occurring by membrane blebbing and tubulation. We show that mutations leading to excess membrane synthesis are sufficient to drive L-form division in *Bacillus subtilis*. Artificially increasing the cell surface area to volume ratio in wild-type protoplasts generates similar shape changes and cell division. Our findings show that simple biophysical processes could have supported efficient cell proliferation during the evolution of early cells and provide an extant biological model for studying this problem.

INTRODUCTION

The peptidoglycan (PG) cell wall is a major defining structure of the bacteria and is present in all known major bacterial lineages. The rare groups of bacteria that lack a wall (e.g., mycoplasma) have probably lost the structure retrospectively. Therefore, the wall was probably present in the last common ancestor of the bacteria, perhaps in the earliest forms of cellular life. Many genes required to make the precursors for cell wall synthesis and assemble them into the meshwork of the growing wall are normally essential for cell viability. This explains why the wall is also such an important target for antibiotics, such as β-lactams and glycopeptides.

In light of the pivotal importance of the wall, it is intriguing that many bacteria are capable of switching into a wall-deficient, or "L-form," state (Allan et al., 2009). Most classically described L-forms were identified as antibiotic-resistant or persistent organisms isolated in association with a wide range of infectious diseases (Domingue and Woody, 1997). Under laboratory conditions, the production of stable L-forms usually requires the inhibition of cell wall synthesis with appropriate antibiotics and long-term passage on osmotically supportive medium to prevent cell lysis (Allan, 1991; Leaver et al., 2009). It has long been known that one or more genetic changes from their parent strain are needed for the formation and/or proliferation of stable L-forms (Allan et al., 2009). Although mutations acquired by L-forms of several organisms have recently been identified by genome sequencing (Briers et al., 2012a; Leaver et al., 2009; Siddiqui et al., 2006), precisely how they contribute to the L-form state remains poorly understood.

The L-form transition results in dramatic changes in cell physiology and morphology because wall synthesis represents a major drain on cellular resources and the wall is essential in determining cell shape. However, the most dramatic change in cell function recognized so far lies in the mode of L-form proliferation. Almost all bacterial cells use a tubulin homolog, FtsZ, to organize a highly ordered ring structure at the site of cell division. This "Z-ring" then recruits about ten other essential division factors, which together drive invagination of a division septum, infill this with new PG, and then organize the orderly separation of the daughter cells (Adams and Errington, 2009; Margolin, 2005). Remarkably, in L-forms, at least in the model system we have developed, this intricate division machinery becomes completely dispensable (Leaver et al., 2009). This is consistent with the finding that L-forms divide not by the precise FtsZ-ring constriction mechanism but by a range of rather poorly regulated shape perturbations, including blebbing, tabulation, and vesiculation (Dell'Era et al., 2009; Kandler and Kandler, 1954; Leaver et al., 2009).

We recently developed a tractable system for studying the cell biology and genetics of L-forms in *Bacillus subtilis* (Domínguez-Cuevas et al., 2012) and used this system to look for genes required specifically for L-form growth (Mercier et al., 2012). We found no evidence for involvement of cytoskeletal proteins in L-form proliferation but instead identified the synthesis of certain branched chain fatty acids as being critical for a late step in separation of progeny cells (scission), suggesting that the precise biophysical properties of the membrane have a crucial role in the proliferation of L-forms.

In this study, we have investigated the mechanisms driving cell division and proliferation of *B. subtilis* L-forms by isolating and studying the effects of mutations that allow cells to proliferate in the L-form state. We find that the key change lies in production of excess membrane by overactivation of the fatty acid synthetic system. This is sufficient to induce shape modulations that progress to scission of progeny cells. Furthermore, artificially increasing the surface area in protoplasts of wild-type cells

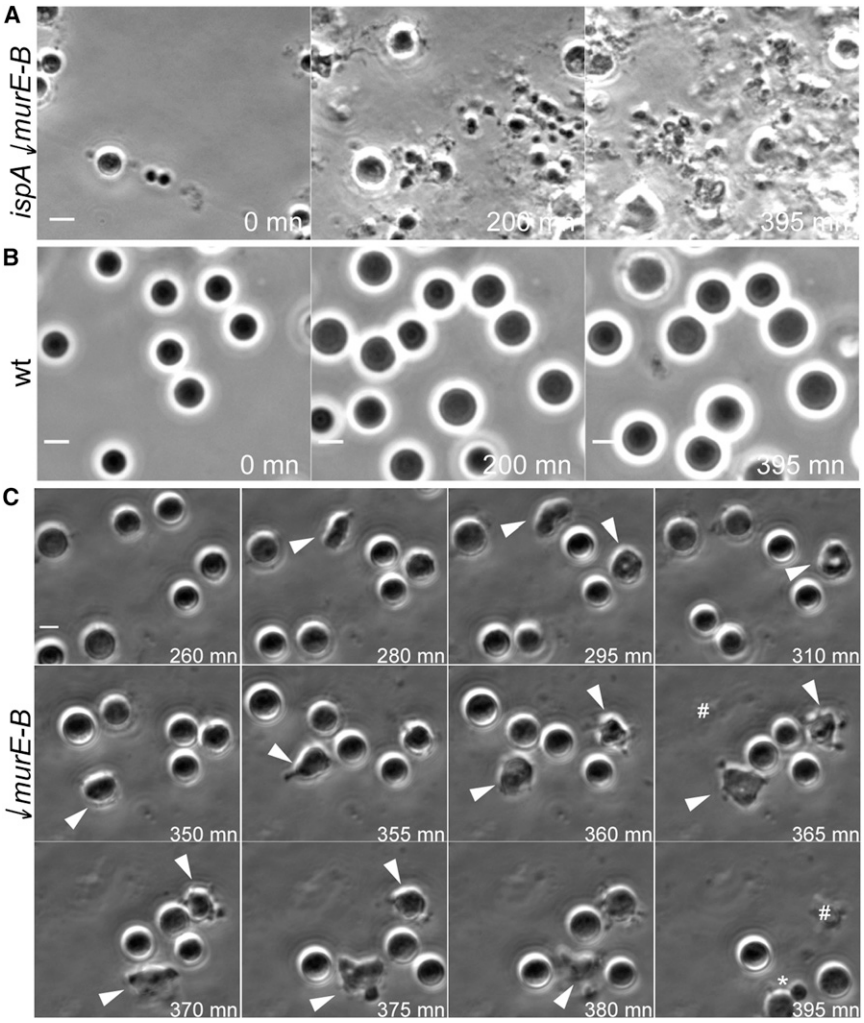

Figure 1. Effects of *ispA* and *murE-B* Mutations on L-Form Growth

(A–C) Strains LR2 (*ispA* P_{xyl}-*murE-B*; A), 168CA (wild-type; B), and Bs115 (P_{xyl}-*murE-B*; C) were grown in the walled state then converted to protoplasts, incubated in L-form-supporting medium (NB/MSM, no xylose) with benzamide (FtsZ inhibitor), and observed by time-lapse phase contrast microscopy. (C) Deformed cells are labeled with arrows, the remains of lysed cells with hashes, and a star points to a successful division event. Elapsed time (min) is shown in each panel.

Scale bars, 3 μm. See also Figure S1 and Movie S1.

generates spontaneous L-form-like shape changes and division. Our results suggest that the division of L-forms is likely due simply to an imbalance between membrane surface area and cellular volume. The findings accord with previous theoretical and in vitro studies of membrane vesicle reproduction aimed at understanding the possible replicative mechanisms of primitive cells (Bozic and Svetina, 2007; Hanczyc et al., 2003; Luisi et al., 2008; Svetina, 2009; Zhu and Szostak, 2009).

RESULTS

Contrasting Effects of *ispA* and P_{xyl}-*murE-B* Mutations on L-Form Growth

We previously showed that repression of the PG precursor pathway using a repressible P_{xyl}-*murE-B* construct, together with a single point mutation of the *ispA* gene encoding a polyisoprenoid synthase, results in L-form growth of *B. subtilis* 168 (Leaver et al., 2009). Consistent with this, complementation of the *ispA* mutation prevented L-form growth in a similar strain (Figure S1A available online). We also built a strain with P_{xyl}-*murE-B* and a repressible allele of *ispA* and showed that this strain also grew well in the L-form state when both promoters were repressed (Figure S1B). Investigations of L-form phenotypes are complicated by several factors: (1) the heterogeneity of the population in terms of cell shape and size; (2) strong selection for compensating mutations that enhance the growth rate or cell stability; and (3) requirement for "escape" mutations that facilitate the emergence of L-forms from a population of rods (Domínguez-Cuevas et al., 2012). To help assess the effects of the different mutations (e.g., repressible *ispA* and P_{xyl}-*murE-B*) on L-form growth, we developed a protocol in which cells of a defined genotype were grown in the rod state, then converted to protoplasts by stripping the cell wall with lysozyme and cultured in our standard L-form medium. The medium contains an osmoprotectant (sucrose) and an inhibitor of cell division (benzamide; Adams et al., 2011) that efficiently kills rods, but not L-forms. For reasons that are not understood, reversion of protoplasts or L-forms to the walled state (regeneration) occurs at a very low frequency, even if they are capable of synthesizing wall material. Benzamide is added to prevent the rare regenerated rods, which grow much more rapidly than L-forms, from overrunning the cultures. Figure 1A (and Movie S1A) shows the transition from protoplasts to proliferating L-forms for strain LR2 (*ispA* P_{xyl}-*murE-B*). In contrast, wild-type cells or *ispA* mutant cells showed only a slow increase in size over many hours (Figure 1B; Movie S1B). Remarkably, even though they showed very little growth and no detectable division, the cells remained intact for many days under these conditions (data not shown). In contrast, after a limited amount of growth, the P_{xyl}-*murE-B* protoplasts frequently initiated L-form-like pulsating shape changes but the cells then lysed. Figure 1C shows a detailed time lapse (from Movie S1C) of a small group of cells over a period of 395 min in L-form medium. Hashes point to the remains of cells that had undergone lysis at some point after the preceding frame. Arrowheads point to these cells in previous frames during

which they exhibited L-form-like shape changes. An asterisk highlights one cell that successfully produced at least one smaller progeny cell (Figure 1C, 395 min). It was evident from these and similar time lapses that these cells are capable of initiating L-form-like shape perturbations and occasionally producing progeny cells, but they do not undergo prolonged proliferative increase because the shape changes are almost always a prelude to cell lysis.

In work to be presented elsewhere, we show that the *ispA* mutation can be substituted by mutations in many genes on different metabolic pathways, albeit generally giving less rapid culture growth than *ispA* (Y.K., R.M., and J.E., unpublished data). We do not yet understand the role of this mutational pathway, although it presumably works at least in part to prevent the cell lysis described for the P_{xyl}-*murE-B* construct and thereby increase the frequency of successful cell division events. In the remainder of this paper, we focus on the P_{xyl}-*murE-B* effect.

Repression of the PG Precursor Pathway Promotes L-Form Growth

In the original experiments of Leaver et al. (2009), we used the P_{xyl}-*murE-B* construct to repress PG precursor synthesis so as to provide an efficient means of converting cells to a wall-deficient state from which growing L-form variants could be isolated. However, the experiments illustrated in Figure 2 show that repression of PG synthesis is required continuously for the efficient growth of L-form cells (in the presence of a lysis-suppressing mutation, in this case, *ispA*). As shown in Figure 2A, repression of the *murE-B* operon allowed vigorous L-form growth, whereas growth was abolished in the presence of inducer. Figure 2B shows that repression of two other genes in the PG precursor pathway, *murC* or *dal*, also allowed L-form growth.

We wished to test whether inhibition of PG precursor synthesis together with an *ispA* (or equivalent) mutation was the only way to generate efficient L-form growth. We took advantage of an improved selection regimen (see Experimental Procedures) to attempt to isolate L-form mutants in a single step, starting from wild-type cells. We succeeded in isolating one such mutant. Genome sequencing revealed that the mutation responsible was an 18 kbp deletion. This deletion removed the *murC* gene, together with 17 other coding regions (Figure 2C). We reconstructed the 18 kbp deletion in the presence of an isopropylthio-β-galactoside (IPTG)-inducible ectopic copy of *murC* on a plasmid (strain RM121) and showed that *murC* is the only essential gene in the deletion (Figure 2D). We then confirmed the ability of this strain to grow as an L-form (Figure 2E). Although we have not fully analyzed this mutant in detail, we assume that deletion of *murC* blocks the PG precursor pathway in a manner similar to depleting MurE-B and that one or more of the nearby deleted genes operates like an *ispA* mutation. Thus, L-form growth under the conditions we use probably requires at least two mutations, and it appeared important that a least one of the mutations blocks the PG precursor pathway.

Overproduction of AccDA Supports L-Form Growth

To better understand the mechanisms underlying the PG precursor effect, we attempted to isolate L-form-promoting mutations that do not affect the PG precursor pathway. Because

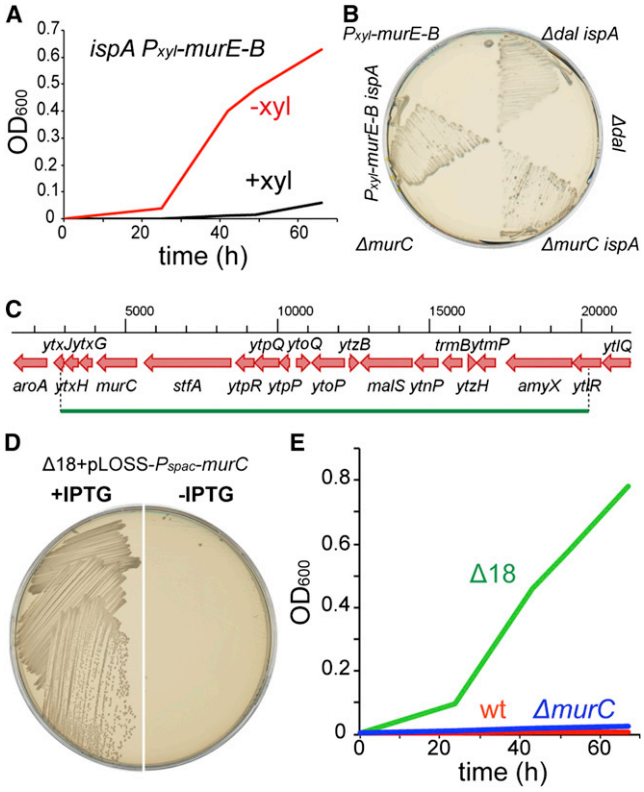

Figure 2. L-Form Growth Requires Mutational Lesions Affecting Two Different Pathways

(A) Strain LR2 (*ispA* P_{xyl}-*murE-B*) was grown in the walled state then converted to protoplasts and incubated in NB/MSM containing benzamide with (+Xyl, black) or without (−Xyl, red) 0.5% xylose.

(B) Growth of strains with the genotypes indicated on NA/MSM plates (to support L-form growth). Strains are Bs115 (P_{xyl}-*murE-B*), LR2 (*ispA* P_{xyl}-*murE-B*), YK1593 (*Δdal*), YK1592 (*ispA Δdal*), RM119 (*ΔmurC*), and YK1409 (*ispA ΔmurC*).

(C) Schematic representation of the chromosomal region deleted in strain RM121 (indicated by the green line).

(D) Growth of the reconstructed strain RM121 containing pLOSS-*erm-murC* (P_{spac}-*murC*) streaked on NA plates in the presence (left) or absence (right) of IPTG.

(E) Growth of protoplasts of strains RM121 (green), *ΔmurC* (blue), and wild-type (red) in L-form-supporting medium (NB/MSM) with benzamide.

mutations blocking this pathway, such as deletion of *murC*, prevent L-forms from reverting to the walled state, we screened for L-form variants that retained the ability to grow as rods (see Experimental Procedures). We started with cells containing an *ispA* mutation to eliminate the need for two mutational events. Revertable mutants were rare but, as shown in Figure 3, we isolated one such mutant, which was able to grow in the walled state, irrespective of the presence or absence of the *ispA* mutation (Figure 3C), and which grew in the L-form state, in the presence of the *ispA* mutation (Figure 3B and 3D; Movie S2). Whole-genome sequencing revealed that the mutant strain RM84 had a single point mutation (*accDA**) (Figure 3A) in the 5′UTR of the operon containing the genes *accD* and *accA*, which together encode the carboxyltransferase subunit of acetyl coenzyme A (CoA) carboxylase (Cronan and Waldrop, 2002).

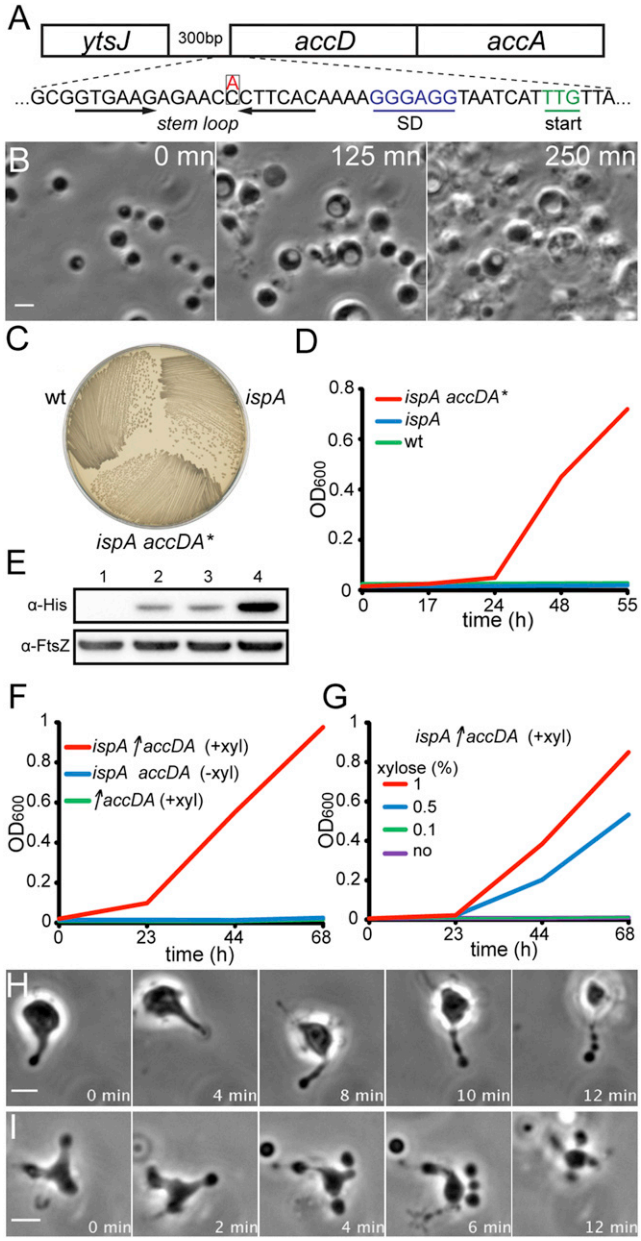

Figure 3. Upregulation of *accDA* Supports L-Form Growth

(A) Schematic representation of the *B. subtilis* genomic region containing the *accDA* genes. The C→A substitution corresponding to the *accDA** mutation is shown in red, the Shine Dalgarno (SD) in blue, and the start codon (start) in green. Arrows indicate the putative stem loop.

(B) Effect of the *accDA** mutation (strain RM84) on growth of protoplasts in L-form-supporting medium (NB/MSM) with benzamide, visualized by time-lapse phase contrast microscopy. Elapsed time (min) is shown in each panel. Scale bar, 3 μm. See also Movie S2.

(C and D) Growth profiles of 168CA (wild-type), RM81 (*ispA*), and RM84 (*ispA accDA**) strains in the walled state (NA plate incubated at 30°C for 24 hr; C) or under L-form conditions (protoplasts incubated 30°C in NB/MSM with benzamide; D).

(E) Western blot analysis of histidine-tagged AccA levels in 168CA (wild-type, lane 1), YK1731 (*accA-his*, lane 2), YK1732 (*ispA accA-his*, lane 3), and YK1733 (*ispA accDA* accA-his*, lane 4). FtsZ levels were also detected as an internal control.

(F and G) Protoplast growth of an *ispA amyE*::P_{xyl}-*accDA* strain (YK1694, red and blue) or an isogenic *ispA*$^+$ strain (YK1738, green) in L-form-supporting medium (NB/MSM) containing benzamide with (red and green) or without (blue) 0.5% xylose (F) or with several different xylose concentrations (YK1694, G). See also Movie S3.

(H and I) Two typical examples of L-form proliferation by strain YK1694 in L-form-supporting medium (NB/MSM) with 0.5% xylose and benzamide, visualized by time-lapse phase contrast microscopy. Elapsed time (min) is shown in each panel. Scale bar, 3 μm.

Because the mutation lay in an inverted repeat just upstream of the *accDA* coding region, it is possible that it works by altering the rate of AccDA synthesis. We tested this possibility by making an *accA-his* fusion gene. Figure 3E shows that the concentration of AccA-His was substantially raised in the presence of the *accDA** mutation (lane 4) and that this was not affected by presence or absence of an *ispA* mutation (lanes 2 and 3). As expected, no signal was seen in the absence of the *his* tag (lane 1). FtsZ was used as an internal control, and its concentration was not affected by any of the mutations (Figure 3E).

To test whether overexpression of AccDA was responsible for the L-form growth phenotype, we constructed a strain carrying an extra copy of *accDA* under the control of xylose-inducible promoter (P_{xyl}) at the ectopic *amyE* locus. We then tested the ability of various protoplasts to grow in L-form medium. As shown in Figure 3F, *accDA* overexpression did indeed induce L-form proliferation in the presence of *ispA* mutation. Figure 3G shows that the rate of growth was dependent on the level of induction of the ectopic copy of *accDA*. In addition, in cells overexpressing AccDA in a wild-type background, time-lapse microscopy revealed shape changes and lysis similar to those observed following PG precursor gene repression (Movie S3). In the presence of the *ispA* mutation, the process of L-form proliferation was also similar to that observed for repression of PG precursor synthesis (Figures 3H and 3I) (Leaver et al., 2009). These results demonstrated that *accDA* overexpression supports L-form growth in much the same way as inhibition of PG precursor synthesis. Control experiments showed that L-form growth was not promoted by overexpression of either gene separately or by overexpression of the *accBC* operon, encoding the biotin carboxylase subunit of acetyl-CoA carboxylase (data not shown).

Overproduction of AccDA Increases the Intracellular Levels of Malonyl-CoA and Fatty Acid Synthase Enzymes

Acetyl-CoA carboxylase, comprising biotin carboxylase (AccBC) and carboxyltransferase (AccDA), carries out the first committed step of fatty acid synthesis: the conversion of acetyl-CoA to malonyl-CoA (Cronan and Waldrop, 2002). In bacteria, fatty acids are synthesized by a repeated cycle of reactions catalyzed by the fatty acid synthase type II enzyme (FAS II) system (Figure 4A) (Rock and Cronan, 1996). The first enzyme in the pathway, FabD, converts malonyl-CoA to malonyl-ACP, the key substrate for the initiation and elongation cycles (Figure 4A) (Rock and Cronan, 1996). The later steps of the FAS II cycle are carried out by proteins, almost all of which are transcriptionally regulated by the FapR repressor in *B. subtilis* (Figure 4A) (Schujman et al.,

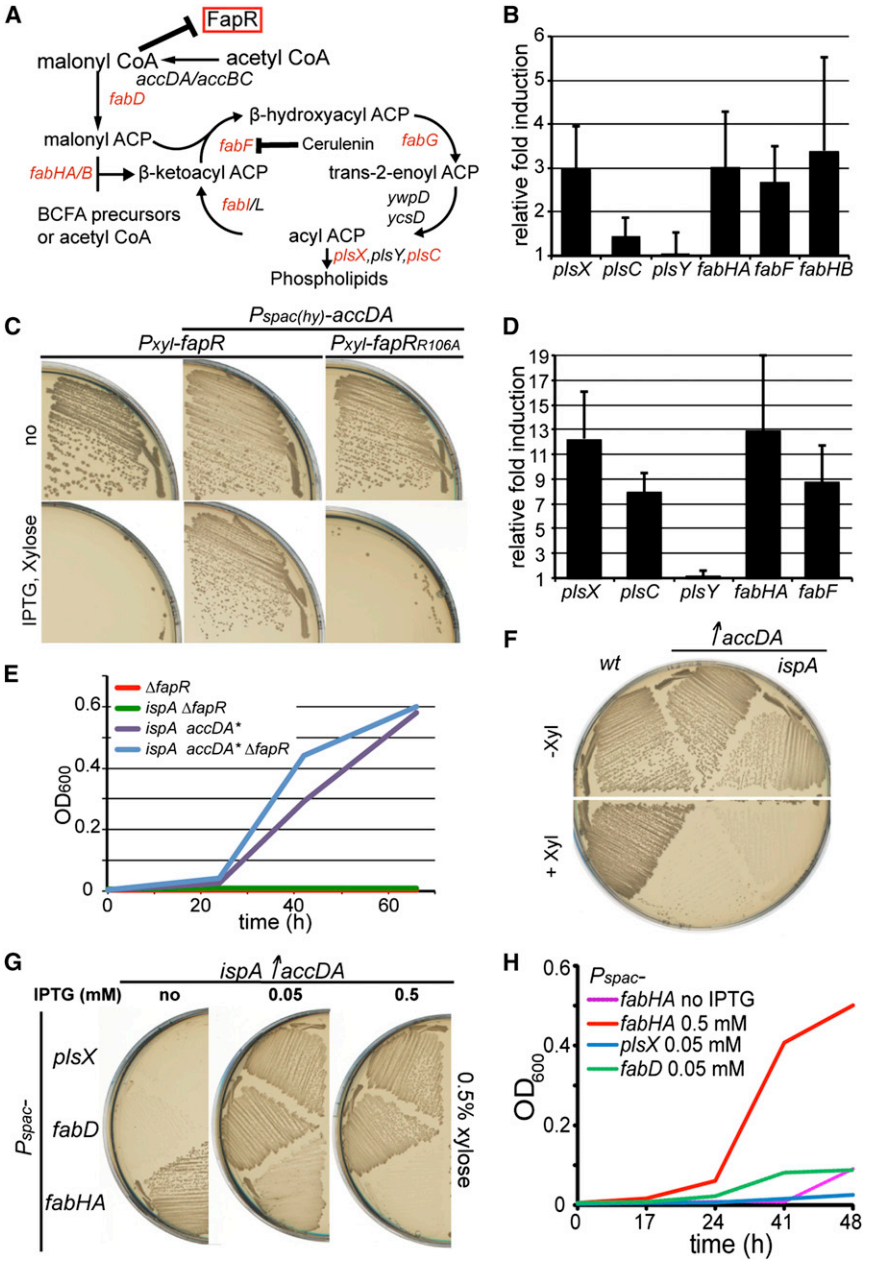

Figure 4. Roles for the FapR Regulator and FAS II Enzyme System in L-Form Growth Promoted by Overexpression of *accDA*

(A) Schematic representation of the *B. subtilis* FAS II system and genes regulated by the FapR protein (red) (after Rock and Cronan, 1996 and Schujman et al., 2003).

(B) Quantitative real-time PCR analysis of the relative change expression of several FapR-regulated genes in an *amyE*::P_{xyl}-*accDA* strain (YK1738) grown in LB with 1% xylose at 37°C. The expression level of each gene is expressed relative to that of a parallel culture without xylose (assigned a value of 1). Mean and SD values (error bars) were calculated using values generated from three independent cultures.

(C) Effect of FapR overexpression on growth in the walled state and its rescue by AccDA overexpression. The following strains were cultured on NA without (top) or with 0.5% xylose and 0.5 mM IPTG (bottom) and incubated for 20 hr at 37°C: *amyE*::P_{xyl}-*fapR* (strain RM208, left), *amyE*::P_{xyl}-*fapR* $P_{spac(hy)}$-*accDA* (YK1726, middle), *amyE*::P_{xyl}-*fapR*$_{R106A}$ $P_{spac(hy)}$-*accDA* (YK1735, right).

(D) Quantitative real-time PCR analysis of the relative change in expression of several FapR-regulated genes in the *ΔfapR* mutant (RM258) grown in LB at 37°C. The expression level of each gene is expressed relative to that of the wild-type (168CA) grown in LB at 37°C as described above (B). Mean and SD values (error bars) were calculated using values generated from three independent cultures.

(E) Protoplast growth in NB/MSM with benzamide of strains carrying the following mutations: *ΔfapR* (strain RM258, red), *ispA ΔfapR* (RM259, green), *ispA accDA** (RM84, purple), *ispA accDA** *ΔfapR* (RM260, blue).

(F) Effect of overproduction of AccDA on growth in the walled state. Strains with the following mutations were cultured on NA plates at 37°C in the presence (bottom) or absence (top) of 0.5% xylose: left, the wild-type (strain 168); middle, *amyE*::P_{xyl}-*accDA* (YK1738); right, *ispA amyE*::P_{xyl}-*accDA* (YK1694).

(G) Effect of repression of FAS II enzyme synthesis on AccDA overexpression lethality. Strains with the following mutations were cultured on NA plates at 37°C in presence of 0.5% xylose (or without; Figure S2E) and with no (left), 0.05 mM (middle), and 0.5 mM (right) IPTG: *ispA amyE*::P_{xyl}-*accDA* with P_{spac}-*plsX* (strain YK1707, top), P_{spac}-*fabD* (YK1710, middle), or P_{spac}-*fabHA* (YK1712, bottom).

(H) Protoplast growth in NB/MSM with 0.5% xylose and benzamide of strains with the following markers and culture supplements: *ispA amyE*::P_{xyl}-*accDA* P_{spac}-*fabHA* without (purple) or with (red) 0.5 mM IPTG and *ispA amyE*::P_{xyl}-*accDA* P_{spac}-*plsX* (blue) or P_{spac}-*fabD* (green) with 0.05 mM IPTG.

See also Figures S2 and S3 and Movies S4 and S5.

2003). Binding of malonyl-CoA to FapR prevents binding of FapR to its target sequences, thereby inducing expression of the *fapR* regulon (Schujman et al., 2003, 2006). Therefore, malonyl-CoA is not only an essential molecular intermediate in the FAS II system but it also plays a key role as a signaling molecule regulating FapR activity to control the synthesis of FAS II components.

It seemed possible that overproduction of AccDA might increase the intracellular levels of malonyl-CoA, which would in turn increase the expression of FAS II genes via relief of FapR repression. To test this possibility, we first examined the effect of AccDA overproduction on expression of the FapR regulon using quantitative PCR (qPCR). As shown in Figure 4B, the expression of various genes in the FapR regulon (but notably not *plsY*, an example of a downstream gene not regulated by FapR) was significantly induced by the overproduction of AccDA. To further investigate the role of FapR, we made a P_{xyl}-*fapR* fusion placed at the *amyE* locus. Xylose-induced ectopic expression of *fapR* strongly inhibited cell viability (normal walled

cells), presumably due to the repression of FAS II components (Figure 4C, left). However, when AccDA was simultaneously overproduced (via an IPTG-inducible construct), the lethality was suppressed (Figure 4C, middle), consistent with increased malonyl-CoA levels relieving the FapR repression. We then made a *fapR* point mutant encoding a protein, $FapR_{R106A}$, with greatly decreased affinity for malonyl-CoA but normal DNA binding activity (Schujman et al., 2006). Synthesis of $FapR_{R106A}$ inhibited cell viability similarly to wild-type FapR, but in this case the growth defect was not suppressed by AccDA overproduction (Figure 4C, right).

These results were consistent with the notion that overproduction of AccDA results in increased levels of malonyl-CoA and that this in turn leads to enhanced FAS II activity via the lifting of FapR repression. To test whether overexpression of the *fapR* regulon was the reason why the overproduction of AccDA promoted L-form growth, we examined the effects of a deletion of *fapR* on protoplast growth. Figure 4D shows that various genes in the *fapR* regulon (but not *plsY*) were, as expected, highly induced in the *ΔfapR* mutant. However, this did not allow protoplasts to grow as L-forms, either in the presence or absence of an *ispA* mutation (Figure 4E). In contrast, L-form growth occurred normally and independent of *fapR* status in cells overproducing AccDA (Figure 4E).

L-Form Growth Promotion Requires Fatty Acid Synthase Activity

During the course of above experiments, we found that the ectopic overexpression of AccDA (*amyE*::P_{xyl}-*accDA*) that supported L-form growth was lethal in the walled state in both wild-type and *ispA* mutant backgrounds (Figures 4F and S2A). In liquid medium, lethality was manifested by culture lysis in the late exponential or early stationary phase (Figures S2B and S2C). These phenotypic effects were again specific for AccDA overproduction and were not seen in the cells overexpressing AccA, AccD, or AccBC (Figure S2D). We wondered whether the lytic phenotype and potentially also the L-form growth capability might be due to excessive fatty acid and/or membrane lipid synthesis. If so, both phenotypes should be dependent on activity of the various FAS II enzymes. We inserted an IPTG-dependent promoter in front of several genes encoding FAS II enzymes. As shown in Figures 4G and S2E, at low levels of IPTG all three constructs supported growth in the walled state on plates, despite the normally lethal effects of AccDA overproduction, presumably due to the reduction in fatty acid synthesis. Indeed, suppression was obtained for the *plsX* and *fabD* constructs even at saturating levels of IPTG (data not shown), suggesting that high levels of their protein products are required for the lethal effect. In the case of the *fabHA* construct, suppression of lethality was only seen in the fully repressed (no-IPTG) state. Note that the *plsX* and *fabD* strains failed to grow at zero IPTG because fatty acid synthesis is of course an essential process in all cells. In contrast, *fabHA* repression was not lethal because it is partially redundant to the *fabHB* gene (Choi et al., 2000). In a complementary experiment, we took advantage of the antibiotic cerulenin, which is a specific inhibitor of FabF (Figure 4A) (Moche et al., 1999). As shown in Figure S2F, the growth inhibition of walled cells caused by overproduction of AccDA was rescued in the presence of sub-MIC levels of cerulenin, which did not affect growth of the wild-type strain.

We then examined the effects of FAS II enzyme repression or inhibition on L-form growth promoted by overproduction of AccDA or inhibition of PG precursor synthesis. Importantly, the same levels of IPTG that suppressed the lethal effects of AccDA overexpression in walled cells were incompatible with growth in the L-form state (Figures 4H and S3A–S3C). A low concentration of cerulenin also blocked growth in the L-form, but not the walled state, and this cerulenin effect was overcome by a resistant allele (*cer-20*; Schujman et al., 1998; Figure S3D). These results strongly suggested that L-form growth is dependent on a threshold level of flux through the fatty acid synthetic pathway.

Consistent with the above, time-lapse experiments showed that L-form proliferation was abolished either by repression of the *plsX* operon (Movie S4) or by treatment with cerulenin (Movie S5). Such cells showed a limited amount of growth reminiscent of wild-type protoplasts. A prevention of cell lysis (*ispA*$^+$ background) was also seen for protoplasts overproducing AccDA when FAS II activity was reduced (data not shown). It therefore seems that activity of the FAS II system is pivotal for L-form proliferation and that the *ispA* mutation pathway acts only to stabilize L-form cells undergoing shape modulation.

AccDA Overproduction Results in Excess Membrane Synthesis

Given the above results, we wished to test more directly for the effects of AccDA overproduction on fatty acid or membrane synthesis. We grew up a strain containing the ectopic xylose-inducible copy of *accDA*, induced with xylose and then stained with a membrane dye (MitoTracker), and examined the cells by fluorescence microscopy. Noninduced cells exhibited the typical rod-shape morphology with a highly regular and smooth fluorescence only associated with the cell surface (Figure 5A). However, in the xylose-treated cells overexpressing AccDA, large irregular patches of staining were evident within many cells (Figure 5B). Interestingly, cell division was slightly impaired for reasons that are not yet clear. A similar phenotype was observed in the *accDA** strain (Figure S4A). By higher-resolution structured illumination microscopy (typical examples and controls in Figures 5C and 5D), the abnormal intracellular staining resolved into what appeared to be closed vesicular structures. We also examined sections of the cells by transmission electron microscopy and again found abnormal intracellular vesicular structures in almost all cells (typical examples and controls in Figures 5E and 5F). Importantly, formation of the abnormal vesicular structures was abolished when FAS II synthesis was downregulated by repression of the P_{spac}-*fabHA* construct (Figure S4B), as in the experiments described above.

These results strongly support the idea that the upregulation of malonyl-CoA synthesis and its increased utilization by the FAS II system, resulting from *accDA* overexpression, leads to excess membrane synthesis.

We also examined the effects of reduced PG precursor synthesis on membrane morphology. Although complete repression of the P_{xyl}-*murE-B* construct is lethal, we found that a low level of xylose (0.1%) allowed a limited degree of growth. As shown in Figure 5G, an excess membrane phenotype similar to

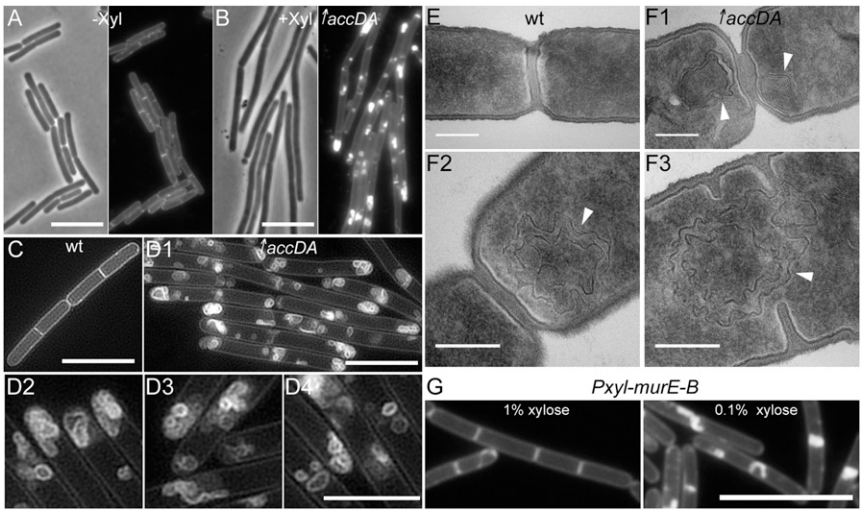

Figure 5. Overexpression of AccDA Results in Excess Membrane Synthesis in Walled *B. subtilis* Cells

(A and B) Phase contrast (left) and corresponding epifluorescence micrographs (right) of strain YK1738 (*amyE*::P_{xyl}-*accDA*), grown in LB with (B) or without (A) 0.5% xylose and stained with the membrane dye MitoTracker green. Scale bar represents 5 μm.

(C and D) N-SIM fluorescence micrographs of wild-type (168CA, C) and YK1738 (*amyE*::P_{xyl}-*accDA*, D1–D4) grown in LB with 0.5% xylose and stained with the membrane dye MitoTracker green. Enlarged images are shown in D2–4. Scale bar represents 5 μm.

(E and F) Transmission electron microscopy images of wild-type (168CA, E) and YK1738 (*amyE*::P_{xyl}-*accDA*, F1–F3) grown in LB with 0.5% xylose. Enlarged images are shown in F2–3. Arrows indicate internal membrane like structures. Scale bar represents 200 nm.

(G) Epifluorescence micrographs of cell membranes stained with the MitoTracker green. Bs115 (P_{xyl}-*murE-B*) was grown in LB with 1% (left) or 0.1% (right) xylose. Scale bar represents 5 μm. *B. subtilis* strains were grown in LB at 37°C (A–G). See also Figure S4.

that generated by overproduction of AccDA was observed. This phenotype was again suppressed by corepression of *fabHA* (Figure S4C).

Excess Membrane Surface Area Is Sufficient to Drive L-Form-like Division in Wild-Type Protoplasts

The above results lead to a simple model in which L-form proliferation is driven by excess membrane synthesis, leading to an abnormal cell surface area to volume (A/V) ratio. If so, artificially increasing the surface area of protoplasts of wild-type (i.e., *accDA*$^+$) cells should lead to spontaneous L-form-like proliferation. We reasoned that a simple way to generate protoplasts with excess surface area was to derive the protoplasts from cells that had been treated with a division inhibitor, thereby generating elongated filaments. When rod-shaped cells elongate, they maintain an almost constant A/V ratio (Figure 6A, red line). However, when such cells are converted to protoplasts, simple geometry dictates that whereas V should remain more or less constant, A will reduce as the cell tends toward an energy-minimizing spherical shape (blue line).

We therefore cultured a wild-type strain for several time periods (0, 30, 60, and 90 min) in the presence of benzamide to generate increasingly elongated cells (Figure 6B). The cells were then treated with lysozyme to generate protoplasts. As shown in Figure 6D1, protoplasts from normal-length rods generated protoplasts with the expected uniform spherical shape. Presumably, the membrane is sufficiently elastic to accommodate relatively small changes in surface area. However, protoplasts with increased cell surface area immediately showed a range of abnormal shapes (Figure 6D2–6D4) reminiscent of L-forms (Figure 6C). Time-lapse imaging revealed that many of the cells went on to divide, generating two or more smaller "progeny" cells; Movie S6 shows the behavior of several cells and cell clusters. Figure 6E shows still images from a typical time course. Undulating shape changes continued for ~15 min, during which time smaller cells pinched off. Eventually (32 min), the shape changes subsided and relatively stable, smaller, and more or less spherical cells remained. The shape changes were most intense in the filaments treated with benzamide for 60 min. In the 90 min sample, the very long filaments were prone to lysis or spontaneous fission during the protoplasting process. Nevertheless, L-form-like shape changes and cell fission were very prominent in all three samples. These proliferative events differed from those of L-forms in that they occurred over a shorter time period and soon subsided. This presumably reflects the fact that the experiment begins with an abrupt and large change in A/V but this soon terminates because cell fission generates increased numbers of smaller cells that "use up" the excess surface area (note that small spheres have a greater A/V ratio than larger spheres; Figure 6A).

DISCUSSION

Two Genetic Changes Required for L-Form Growth

The natural history of bacterial L-forms has been extensively described in the literature (Allan et al., 2009; Domingue and Woody, 1997), but until recently almost nothing was known about the molecular mechanisms underlying L-form proliferation. In this paper, we show that under our standard experimental conditions, two genetic changes are needed for L-form growth in *B. subtilis*. One mutation is needed to oversynthesize membrane fatty acids and can occur directly, by upregulating the FAS II system via AccDA overproduction, or indirectly, via inhibition of the PG precursor pathway. A single point mutation in a stem-loop structure just upstream of *accD* coding region increased intracellular levels of AccDA, suggesting that a regulatory mechanism controlling AccDA synthesis may exist in *B. subtilis*. Little is known about how PG synthesis is coordinated with either membrane synthesis or cell growth. Interestingly, we found that inhibition of PG precursor synthesis also promotes excess

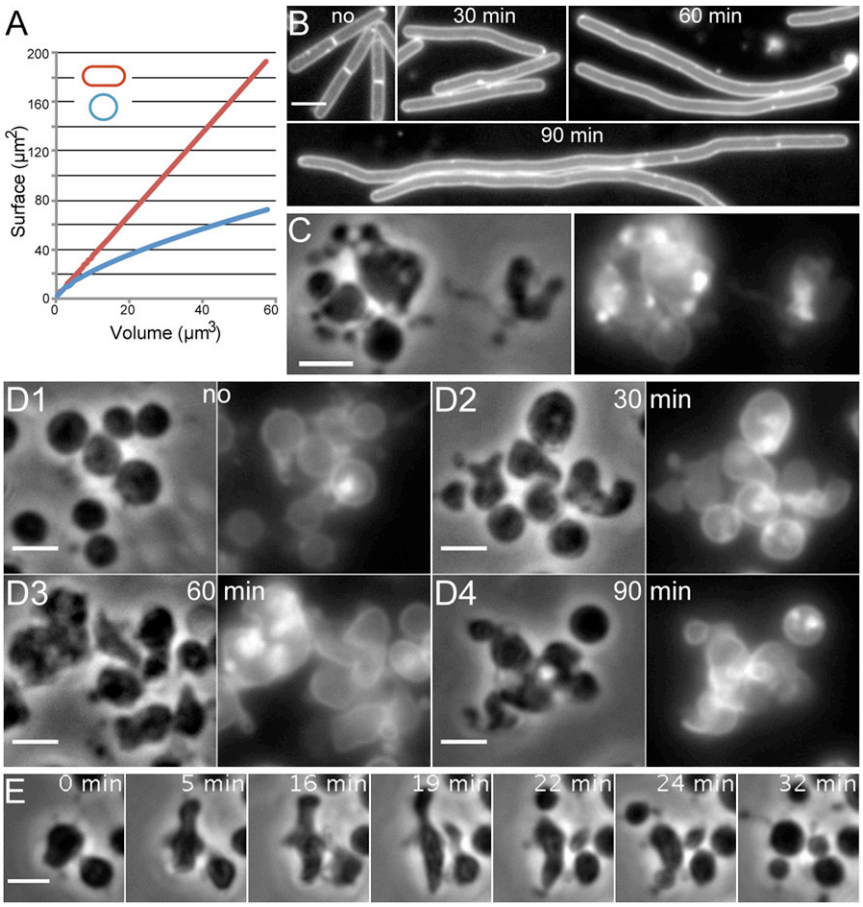

Figure 6. Excess Membrane Promotes Shape Changes and Membrane Scission in Protoplasts

(A) Theoretical relationship between surface area and volume in rod-shaped (red) or spherical (blue) cells.

(B) Epifluorescence microscopy of rod-shaped cells of the strain 168CA (wild-type), stained with the membrane dye Nile red, after treatment with benzamide for various time periods (30, 60, and 90 min) or without (no).

(C) Exponentially growing L-form culture of YK1694 (*ispA amyE::*P_{xyl}*-accDA*) in NB/MSM with 0.5% xylose and benzamide.

(D) Phase contrast and corresponding epifluorescence microscopy of cells with increased volume, corresponding to (B), immediately after treatment with lysozyme, leading to their conversion into protoplasts. Cells were stained with the membrane dye Nile red.

(E) Effect of the increased surface area of wild-type protoplast on membrane scission, visualized by time-lapse phase contrast microscopy. Exponentially growing wild-type (168CA) cells in LB were treated with benzamide for 60 min and then obtained filamentous rod cells were treated with lysozyme. Elapsed time (min) after the period of treatment with lysozyme is shown in each panel. See also Movie S6. Scale bars represent 3 μm See also Figure S5.

membrane synthesis. This suggests that membrane lipid synthesis is negatively regulated by some element of the PG precursor synthesis pathway. However, such regulation seems indirect because no significant effects on intracellular levels of AccDA were seen following the inhibition of PG precursor synthesis (Figure S3E). Given that L-forms are viable in the absence of PG precursor synthesis, they may provide an interesting experimental vehicle for studying the apparent regulatory interplay between membrane and wall synthesis.

Interestingly, Bendezú and de Boer (2008) recently showed that when *E. coli* cultures are mutationally induced to switch from rods to spheres they fail to compensate for the changes in A/V ratio and continue to produce membrane at the higher rate required for rod-shaped cells. These mutants then generate intracellular vesicles when cell division is inhibited and cell size increases, presumably due to the excess membrane (Bendezú and de Boer, 2008). However, no such excess membrane phenotype was seen when normal-sized *B. subtilis* rods were converted to spherical protoplasts (Figure 6D1). Moreover, no vesicles were observed in an equivalent *B. subtilis* round (*rodA*) mutant after inhibition of cell division (Figure S5A). However, vesicles did appear in the *rodA* mutant when membrane synthesis was elevated by AccDA overproduction (Figure S5B). Therefore, it seems that, unlike *E. coli*, *B. subtilis* can at least partially adapt its rate of membrane synthesis to accommodate changes in A/V.

It now seems that the *ispA* mutation previously reported to sustain L-form growth (Leaver et al., 2009) works by somehow stabilizing L-form cells undergoing shape modulation. We will report in more detail on this effect elsewhere (Y.K., R.M., and J.E., unpublished data). IspA catalyzes the formation of farnesyl pyrophosphate in the polyprenoid synthetic pathway (Julsing et al., 2007). This pathway leads to the formation of two essential lipid molecules: menaquinone, involved in the respiratory chain, and bactoprenol, required for synthesis of both peptidoglycan and teichoic acids. Recent papers have described the isolation and characterization of L-forms of *Listeria monocytogenes*, a close relative of *B. subtilis* (Briers et al., 2012a; Dell'Era et al., 2009). Although the proliferation of *L. monocytogenes* L forms appears different in morphological detail to *B. subtilis*, we note first that the culture conditions used in the *Listeria* experiments were very different (cells embedded in soft agar) from those used here (liquid medium), and second that the genome sequence of a *Listeria* L-form isolate apparently contained a mutation in the gene encoding 3-hydroxy-3-methylglutaryl-CoA synthase, which participates in polyprenoid precursor synthesis and might therefore operate in a similar manner to *ispA* of *B. subtilis*.

Excess Membrane as a Mechanistic Driver for L-Form Division

L-forms proliferate by an unusual membrane deformation and scission process that is completely independent of the normally essential FtsZ-based cell division machinery in *B. subtilis* (Leaver

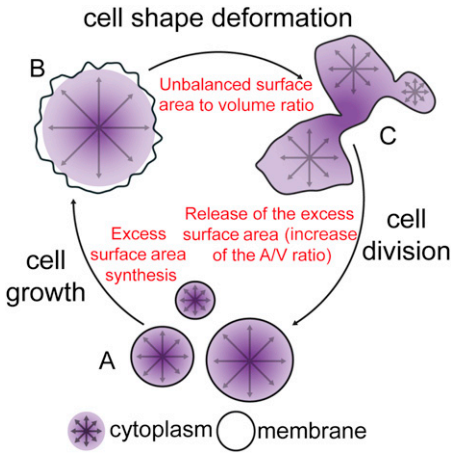

Figure 7. A Model for Proliferation of L-Form Cells

(A–C) Newborn L-forms (A) grow in an unbalanced manner with excess surface area (membrane) synthesis. The excess surface area (B) drives shape deformation (C). Scission of lobes or blebs of cytoplasm generates smaller progeny cells in which the area/volume ratio is normalized by simple geometric effects. See text for a full description.

et al., 2009) and they also do not require any of the currently known cytoskeletal systems (Mercier et al., 2012). Chen (2009) has pointed out that L-form division might occur by purely biophysical processes, and in our previous paper (Mercier et al., 2012) we showed that a late stage in proliferation is dependent on a particular membrane composition, probably associated with high membrane fluidity. The results described here strongly suggest that an imbalance between cell membrane and volume growth drives the cell shape deformations leading to scission and thus L-form proliferation. This conclusion is based on the following key observations: (1) overproduction of AccDA, leading to excess membrane synthesis, is sufficient for L-form growth and proliferation; (2) a partial decrease in flux through the FAS II system can block L-form proliferation without affecting growth of walled cells; and (3) artificially increasing cell surface area by the conversion of elongated rods to protoplasts is sufficient to produce L-form-like shape changes and scission in wild-type cells. Figure 7 summarizes our new view of the process of L-form proliferation in *B. subtilis*. In step one (1), unbalanced growth generates an increase in cell surface area relative to cytoplasmic volume. The resultant torsional stress then leads to spontaneous shape deformation (2). The deformed cell then resolves spontaneously (scission) into discrete progeny cells. The total surface area of several small cells is greater than that of a single cell of equal total volume and similar shape, so the disequilibrium between surface area and volume can be corrected by progeny formation (3). Repetition of this cycle leads to indefinite L-form proliferation.

L-Forms as a Model for Proliferation in Primitive Cell

It has been suggested that L-forms might represent a useful model system for the study of bacterial evolution and ancestry (Briers et al., 2012a; Leaver et al., 2009; Mercier et al., 2012). Several in vitro studies have demonstrated proliferation in relatively simple vesicle systems without the intervention of protein-based mechanisms (Hanczyc et al., 2003; Peterlin et al., 2009; Terasawa et al., 2012; Zhu and Szostak, 2009). The in vitro replication methods mentioned above all rely in one way or another on achieving an imbalance between vesicle surface area and internal volume. Furthermore, the theoretical basis for generation of shape changes, pinching and budding of vesicles, by this mechanism, has been well documented (Bozic and Svetina, 2007; Luisi et al., 2008; Svetina, 2009). Similarly, L-form proliferation in *B. subtilis* does not require the mechanisms that are pivotal for regulation of cell division, cell shape, elongation, coordinated chromosome segregation, and balanced membrane lipid synthesis of walled cells (Leaver et al., 2009; Mercier et al., 2012), but it does requires excess membrane production to generate an imbalance between growth of cell surface area and volume. In addition, although various modes of cell division have been described for proliferation of L-forms, including membrane extrusion, blebbing, and vesiculation (reviewed recently in Briers et al., 2012b and Errington, 2013), all of these events seem to be achievable in relatively simple in vitro lipid vesicle systems (Hanczyc et al., 2003; Peterlin et al., 2009; Terasawa et al., 2012; Zhu and Szostak, 2009). Our results provide direct support for the notion that purely biophysical effects could have supported an efficient mode of proliferation in primitive cells, before the invention of the cell wall, and provide an extant model for exploration of the possible properties of early forms of cellular life.

EXPERIMENTAL PROCEDURES

Bacterial Strains, Plasmids, and Growth Conditions

The bacterial strains and plasmid constructs used in this study are shown in Table S1. DNA manipulations and *E. coli* DH5α transformation were carried out using standard methods (Sambrook et al., 1989). Transformation of competent *B. subtilis* cells was performed by the two-step starvation procedure as previously described (Anagnostopoulos and Spizizen, 1961; Hamoen et al., 2002). *E. coli* and normal *B. subtilis* cells were grown on nutrient agar (NA, Oxoid) and in Luria-Bertani broth (LB). *B. subtilis* L-forms were grown in osmoprotective medium composed of 2 × magnesium-sucrose-maleic acid (MSM) pH 7 (40 mM $MgCl_2$, 1 M sucrose, and 40 mM maleic acid) mixed 1:1 with 2 × nutrient broth (NB, Oxoid) or 2 × NA. DM3 medium (pH 7.3; 0.5 M succinate, 0.5% casamino acids, 0.5% yeast extract, 0.5% glucose, 0.35% K_2HPO_4, 0.15% KH_2P0_4, 20 mM $MgCl_2$, 0.01% bovine serum albumin, and 1% agar) (Bourne and Dancer, 1986) was used to regenerate cell wall from *B. subtilis* L-forms. Supplements, xylose and IPTG, were added as needed at the concentration indicated. When necessary, antibiotics were added to media at the following concentrations: cerulenin, 2 μg/ml or 10 μg/ml; ampicillin, 100 μg/ml; chloramphenicol, 5 μg/ml; kanamycin, 5 μg/ml; spectinomycin, 50 μg/ml; erythromycin, 1 μg/ml or 0.2 μg/ml; and tetracycline, 10 μg/ml. Benzamide (1 μg/ml, FtsZ inhibitor 8J; Adams et al., 2011) was used for protoplast growth experiments to prevent the growth of walled cells.

Protoplast Preparation and Growth

Protoplasts were prepared as described by Domínguez-Cuevas et al. (2012). Briefly, an exponential cell culture (optical density 600 nm [OD_{600nm}] of 0.2) was harvested and resuspended in NB/MSM medium containing lysozyme (500 μg/ml) and benzamide. After incubation at 37°C with shaking for 1h, the cell cultures were diluted at 10^{-3} into fresh NB/MSM containing benzamide and supplements, if required. The cell cultures were incubated at 30°C without shaking and samples were removed about every 12 hr for measurement.

Selection of Mutations Promoting L-Form Proliferation

For selection of the RM121 mutant, a protoplast suspension of strain 168CA were diluted at 10^{-2} into fresh NB/MSM containing benzamide and incubated at 30°C without shaking for several days. Genomic DNA of a proliferating

L-form culture (as judged by phase contrast microscopy) was extracted and the mutations were identified by whole-genome sequencing.

For the selection of the *accDA** mutant, protoplasts of strain RM81 (*ispA*) were diluted at 10^{-2} into fresh NB/MSM containing benzamide and incubated at 30°C without shaking for several days. Proliferating L-form cultures (as judged by phase contrast microscopy) were diluted at 10^{-3} into fresh medium and incubated at 30°C for 3 days. After several dilution cycles, purified L-form cultures were diluted at 10^{-3} in the protoplast regeneration DM3 medium and incubated at 30°C for 3 days. Regenerated (walled) rod-shape cell cultures were chosen and the intrinsic ability of these mutants to grow as L-forms was monitored by protoplasting and transfer back into L-form medium (NB/MSM). Genomic DNA of the selected mutants was extracted and the mutations were identified by whole-genome sequencing.

Genome Sequencing and Identification of Single-Nucleotide Polymorphisms

Whole-genome sequencing was performed with the Illumina HiSeq 2000 System (GATC-Biotech, Germany). Sequencing samples were prepared as described previously (Domínguez-Cuevas et al., 2012). Sequence reads were aligned with SeqMan Ngen (DNASTAR, Madison, WI, USA) software using the National Center for Biotechnology Information *B. subtilis* 168 genome (GenBank: AL009126.3) as reference. Single-nucleotide polymorphisms and nucleotides deletion/insertion were analyzed with SeqMan Pro (DNASTAR) software.

Western Blot and Quantitative Real-Time PCR

The intracellular concentrations of FtsZ or histidine-tagged AccA were determined using western blot analyses as previously described (Ishikawa et al., 2006). *B. subtilis* cells were grown in LB medium at 37°C, and at an OD_{600} of 0.5 a 10 ml sample was taken. After centrifugation, the cells were lysed by lysozyme, mixed with SDS sample buffer, heat denatured, and loaded onto SDS-polyacrylamide gel for western blot analysis.

For quantitative real-time PCR, cultures were grown in 5 ml LB medium with or without appropriate supplements at 37°C. Cell samples were harvested at an OD_{600nm} of 0.8, and total RNA was isolated and retrotranscribed (1 μg) as previously described (Domínguez-Cuevas et al., 2012). Complimentary DNA (cDNA) samples were diluted 1:80. A total of 4 μl cDNA was added to 10 μl MESA Blue qPCR Master Mix Plus (Eurogentec), 2 μl of each primer (1 μM stock), and 2 μl H_2O. qPCR was performed on a Rotor-Gene Q cycler (QIAGEN) with 40 cycles of 5 s at 95°C and 60 s at 60°C. Cycle and threshold were obtained according to the manufacturer's instructions. Control genes (*noc* and *soj*) were used as references for comparison with the genes of interest. Changes in expression given are the average of three biological replicates.

Microscopy and Image Analysis

For time-lapse microscopy, *B. subtilis* L-form cells were imaged in ibiTreat-adherent 35 mm sterile glass-bottom microwell dishes (ibidi GmbH, Munich, Germany). Cells were prepared as previously described (Mercier et al., 2012). The cells were imaged on a DeltaVision RT microscope (Applied Precision, Issaquah, WA, USA) controlled by softWoRx (Applied Precision) with a Zeiss ×100 apofluor oil-immersion lens. A Weather Station environmental chamber (Precision Control) regulated the temperature of the stage.

For fluorescence microscopy, a late exponential phase culture of *B. subtilis* grown on LB at 37°C was stained with MitoTracker green. After several washings with fresh LB, the cells were mounted on microscope slides covered with an agarose pad. The cells were imaged on a Zeiss Axiovert 200 M microscope equipped with a Sony Cool-Snap HQ cooled CCD camera or on a Nikon N-SIM microscope equipped with a Nikon APO TIRF ×100/1.49 lens in both EPI and 2D-SIM modes with 488 nm solid-state lasers.

For electron microscopy, a late exponential phase culture of *B. subtilis* grown on LB at 37°C was fixed with 2% gluteraldehyde in sodium cacodylate buffer and secondarily fixed with 1% osmium tetroxide and potassium ferricyanide. The dehydration, embedding, sectioning, and staining were performed by the Electron Microscopy Research Services Unit (Newcastle University). The grids were examined on a Philips CM 100 Compustage (FEI) transmission electron microscope and digital images were collected using an AMT CCD camera (Deben).

Pictures and movies were prepared for publication using ImageJ (http://rsb.info.nih.gov/ij) and Adobe Photoshop.

Theoretical Cell Volume and Surface Area Considerations

As described in Bendezú and de Boer (2008), the volume (V) and surface area (S) of a rod-shaped cell were calculated using $V_r = 4/3\pi r^3 + \pi r^2 h$, $S_c = 4\pi r^2 + 2\pi rh$, with r the radius and h the cell length. r was measured from *B. subtilis* cells grown in NB/MSM. The volume and surface area of a spherical cell were calculated using $V_s = 4/3\pi r^3$, $S_s = 4\pi r^2$.

SUPPLEMENTAL INFORMATION

Supplemental Information includes five figures, six movies, and one table and can be found with this article online at http://dx.doi.org/10.1016/j.cell.2013.01.043.

ACKNOWLEDGMENTS

We thank Henrik Strahl for technical support and extensive discussions and Patricia Domínguez-Cuevas, Waldemar Vollmer, and Ling Juan Wu for critical reading of the manuscript. We thank Donald Zeigler (BGSC) for strain OBS20. This work was funded by European Research Council Advanced Investigator grant 250363 ("OPAL"; to J.E.). R.M. was supported by EMBO Long Term and Marie-Curie Intra-European Fellowships.

Received: August 25, 2012
Revised: December 12, 2012
Accepted: January 24, 2013
Published: February 28, 2013

REFERENCES

Adams, D.W., and Errington, J. (2009). Bacterial cell division: assembly, maintenance and disassembly of the Z ring. Nat. Rev. Microbiol. *7*, 642–653.

Adams, D.W., Wu, L.J., Czaplewski, L.G., and Errington, J. (2011). Multiple effects of benzamide antibiotics on FtsZ function. Mol. Microbiol. *80*, 68–84.

Allan, E.J. (1991). Induction and cultivation of a stable L-form of *Bacillus subtilis*. J. Appl. Bacteriol. *70*, 339–343.

Allan, E.J., Hoischen, C., and Gumpert, J. (2009). Bacterial L-forms. Adv. Appl. Microbiol. *68*, 1–39.

Anagnostopoulos, C., and Spizizen, J. (1961). Requirements for transformation in *Bacillus subtilis*. J. Bacteriol. *81*, 741–746.

Bendezú, F.O., and de Boer, P.A. (2008). Conditional lethality, division defects, membrane involution, and endocytosis in mre and mrd shape mutants of *Escherichia coli*. J. Bacteriol. *190*, 1792–1811.

Bourne, N., and Dancer, B.N. (1986). Regeneration of protoplasts of *Bacillus subtilis* 168 and closely related strains. J. Gen. Microbiol. *132*, 251–255.

Bozic, B., and Svetina, S. (2007). Vesicle self-reproduction: the involvement of membrane hydraulic and solute permeabilities. Eur Phys J E Soft Matter *24*, 79–90.

Briers, Y., Staubli, T., Schmid, M.C., Wagner, M., Schuppler, M., and Loessner, M.J. (2012a). Intracellular vesicles as reproduction elements in cell wall-deficient L-form bacteria. PLoS ONE *7*, e38514.

Briers, Y., Walde, P., Schuppler, M., and Loessner, M.J. (2012b). How did bacterial ancestors reproduce? Lessons from L-form cells and giant lipid vesicles: multiplication similarities between lipid vesicles and L-form bacteria. Bioessays *34*, 1078–1084.

Chen, I.A. (2009). Cell division: breaking up is easy to do. Curr. Biol. *19*, R327–R328.

Choi, K.H., Heath, R.J., and Rock, C.O. (2000). beta-ketoacyl-acyl carrier protein synthase III (FabH) is a determining factor in branched-chain fatty acid biosynthesis. J. Bacteriol. *182*, 365–370.

Cronan, J.E., Jr., and Waldrop, G.L. (2002). Multi-subunit acetyl-CoA carboxylases. Prog. Lipid Res. *41*, 407–435.

Dell'Era, S., Buchrieser, C., Couvé, E., Schnell, B., Briers, Y., Schuppler, M., and Loessner, M.J. (2009). *Listeria monocytogenes* L-forms respond to cell wall deficiency by modifying gene expression and the mode of division. Mol. Microbiol. *73*, 306–322.

Domingue, G.J., Sr., and Woody, H.B. (1997). Bacterial persistence and expression of disease. Clin. Microbiol. Rev. *10*, 320–344.

Domínguez-Cuevas, P., Mercier, R., Leaver, M., Kawai, Y., and Errington, J. (2012). The rod to L-form transition of *Bacillus subtilis* is limited by a requirement for the protoplast to escape from the cell wall sacculus. Mol. Microbiol. *83*, 52–66.

Errington, J. (2013). L-form bacteria, cell walls and the origins of life. Open Biol. *3*, 120143.

Hamoen, L.W., Smits, W.K., de Jong, A., Holsappel, S., and Kuipers, O.P. (2002). Improving the predictive value of the competence transcription factor (ComK) binding site in *Bacillus subtilis* using a genomic approach. Nucleic Acids Res. *30*, 5517–5528.

Hanczyc, M.M., Fujikawa, S.M., and Szostak, J.W. (2003). Experimental models of primitive cellular compartments: encapsulation, growth, and division. Science *302*, 618–622.

Ishikawa, S., Kawai, Y., Hiramatsu, K., Kuwano, M., and Ogasawara, N. (2006). A new FtsZ-interacting protein, YlmF, complements the activity of FtsA during progression of cell division in *Bacillus subtilis*. Mol. Microbiol. *60*, 1364–1380.

Julsing, M.K., Rijpkema, M., Woerdenbag, H.J., Quax, W.J., and Kayser, O. (2007). Functional analysis of genes involved in the biosynthesis of isoprene in *Bacillus subtilis*. Appl. Microbiol. Biotechnol. *75*, 1377–1384.

Kandler, G., and Kandler, O. (1954). [Studies on morphology and multiplication of pleuropneumonia-like organisms and on bacterial L-phase, I. Light microscopy]. Arch. Mikrobiol. *21*, 178–201.

Leaver, M., Domínguez-Cuevas, P., Coxhead, J.M., Daniel, R.A., and Errington, J. (2009). Life without a wall or division machine in *Bacillus subtilis*. Nature *457*, 849–853.

Luisi, P.L., de Souza, T.P., and Stano, P. (2008). Vesicle behavior: in search of explanations. J. Phys. Chem. B *112*, 14655–14664.

Margolin, W. (2005). FtsZ and the division of prokaryotic cells and organelles. Nat. Rev. Mol. Cell Biol. *6*, 862–871.

Mercier, R., Domínguez-Cuevas, P., and Errington, J. (2012). Crucial role for membrane fluidity in proliferation of primitive cells. Cell Rep. *1*, 417–423.

Moche, M., Schneider, G., Edwards, P., Dehesh, K., and Lindqvist, Y. (1999). Structure of the complex between the antibiotic cerulenin and its target, beta-ketoacyl-acyl carrier protein synthase. J. Biol. Chem. *274*, 6031–6034.

Peterlin, P., Arrigler, V., Kogej, K., Svetina, S., and Walde, P. (2009). Growth and shape transformations of giant phospholipid vesicles upon interaction with an aqueous oleic acid suspension. Chem. Phys. Lipids *159*, 67–76.

Rock, C.O., and Cronan, J.E. (1996). *Escherichia coli* as a model for the regulation of dissociable (type II) fatty acid biosynthesis. Biochim. Biophys. Acta *1302*, 1–16.

Sambrook, J., Fritsch, E.F., and Maniatis, T. (1989). Molecular Cloning: A Laboratory Manual (Cold Spring Harbor: Cold Spring Harbor Laboratory Press).

Schujman, G.E., Grau, R., Gramajo, H.C., Ornella, L., and de Mendoza, D. (1998). De novo fatty acid synthesis is required for establishment of cell type-specific gene transcription during sporulation in *Bacillus subtilis*. Mol. Microbiol. *29*, 1215–1224.

Schujman, G.E., Paoletti, L., Grossman, A.D., and de Mendoza, D. (2003). FapR, a bacterial transcription factor involved in global regulation of membrane lipid biosynthesis. Dev. Cell *4*, 663–672.

Schujman, G.E., Guerin, M., Buschiazzo, A., Schaeffer, F., Llarrull, L.I., Reh, G., Vila, A.J., Alzari, P.M., and de Mendoza, D. (2006). Structural basis of lipid biosynthesis regulation in Gram-positive bacteria. EMBO J. *25*, 4074–4083.

Siddiqui, R.A., Hoischen, C., Holst, O., Heinze, I., Schlott, B., Gumpert, J., Diekmann, S., Grosse, F., and Platzer, M. (2006). The analysis of cell division and cell wall synthesis genes reveals mutationally inactivated ftsQ and mraY in a protoplast-type L-form of *Escherichia coli*. FEMS Microbiol. Lett. *258*, 305–311.

Svetina, S. (2009). Vesicle budding and the origin of cellular life. ChemPhysChem *10*, 2769–2776.

Terasawa, H., Nishimura, K., Suzuki, H., Matsuura, T., and Yomo, T. (2012). Coupling of the fusion and budding of giant phospholipid vesicles containing macromolecules. Proc. Natl. Acad. Sci. USA *109*, 5942–5947.

Zhu, T.F., and Szostak, J.W. (2009). Coupled growth and division of model protocell membranes. J. Am. Chem. Soc. *131*, 5705–5713.